Optical and Quantum Electronics (2024) 56:9
https://doi.org/10.1007/s11082-023-05577-z

Effect of ZnO doping co-carried out by Co–Cu on nonlinear optical properties prepared by the spin coating method

Abdelkader Mohammedi[1,2] · Omar Meglali[2,3] · Miloud Ibrir[1,2] · Bernabé Marí[4] · R. Peña-Garcia[5,6] · Nadir Bouarissa[1,2]

Received: 12 May 2023 / Accepted: 11 October 2023

Abstract
In the present work, thin films of ZnO co-doped with Co and Cu cations were obtained on glass substrate, combining the sol gel process and spin-coating technique. For the compound, the general chemical formula used was: $Zn_{1-x-z}Co_xCu_zO$, [(x; z) = (0.00; 0.00), (0.02; 0.02), (0.04; 0.04) and (0.06; 0.06)]. For pure ZnO film, the surface morphology is composed by small spherical grains that present interstitial spaces, while the films obtained from the simultaneous Co and Cu insertion in the ZnO structure are more dense and interstitial spaces disappear. For all films, the X-ray diffraction patterns testify the monophasic phase formation, typical of the hexagonal structure of ZnO. In addition, the films presented preferential orientation in the (002) direction. It was demonstrated that the Zn^{2+} cations by Co^{2+} and Cu^{2+} cations replacement, causes relevant modifications in the lattice parameter (c), crystallite size (D), dislocation density (δ), strain (ε_c) and stress (σ_c) of the hexagonal structure wurtzite from ZnO. The Co and Cu cations inclusion in the ZnO host lattice, alto caused a decrease in the optical band gap energy (3.37 for 3.16 eV), which is related to the charge transfer between the 4f level electrons and the conduction band or valence band of ZnO. Finally, for all films thin the linear and non-linear optical constants were computed and analyzed, showing variations that depend on the concentration of the dopant cations.

Keywords (Co–Cu) co-doped ZnO · Thin films · Sol–gel process · Spin coating · XRD patterns

1 Introduction

The importance of linear and non-linear optical semiconductors (NLOs) lies in the optical properties within which light is propagated. Therefore, they are used in various applications such as: optical waveguides, optoelectronic apparatuses, optical switching, image treatment, optical signal processing, optical enquiry stocking, optical locating, high-speed optical connections, and after time appliances in biological and medical sciences (Nagaraja et al. 2013).

Zinc oxide (ZnO) thin films are extensively studied because they have high photoelectric possessions, high electrochemical stability andenergy gap ($E_g = 3.37$eV) at

Extended author information available on the last page of the article

room temperature (Yan et al. 2020). The ZnO doped and codoped with different cations is inspected as an excellent strategy for changes and improves various physical properties such as, crystalline quality, reducing crystal defects and modulating the energy gap (Kompa et al. 2023; Andriotis and Menon 2015; Chaitra et al. 2017; Mohammedi et al. 2022). The ZnO properties have been studied from the insertion of a simple cations: Fe(Hadimani et al. 2018), Mg(Mahroug et al. 2019), Ni (Oudjertli et al. 2022), Al (Islam et al. 2019), Cu (Mohammedi et al. 2021), Al, Cu, Co and In (Kim et al. 2015), and with two simultaneous cations such as: (Co–Al) and (Ni–Cu) (Swapna and Reddy 2018; Ali et al. 2018), (Y–Fe) (Peña-Garcia et al. 2020), (Ni–Sr) (Peña-Garcia et al. 2019), (Fe–Pr) (Rocha et al. 2023), (Ni–Ce) (Costa-Silva et al. 2022) and (Er–Cr) (França et al. 2023) Also, Goktas et al. (2018) reported the structural, optical and magnetic properties Co–Cu doped ZnO thin films that was annealed in air and argon atmosphere. The NLOand ZnO thin films doped with Na (Deekshitha et al. 2019), Zr (Bahedi et al. 2009a), and Ce (Chen et al. 2020) have demonstrated optical improved properties (Peng et al. 2018).

Other simple oxides, such as CoO, have been studied by Z-Scan by various researchers (Chouhan et al. 2017). Also, the study of NLO properties of ZnO structures by Z-Scan has been madeby different authors (Mostafa et al. 2021). For example, Mustafa et al. examined the NLO properties of ZnO samples doped and co-doped with Zn and Ag prepared with PLD technique. They reported an enhancement in the NLO properties for the Ag/Zn/ZnO co-doped sample, which may be suitable for optical applications (Ali et al. 2018). Furthermore, non-linear optical response $\chi^{(3)} = 20.12 \times 10^{-12}$ on Zr- doped ZnO films utilizing the spray pyrolysis technique was reported (Bahedi et al. 2009b)**.**

Based on this argument, in this work, Co-Cuco-doped ZnO thin films have been obtained on glass substrate, combining the sol–gel method and spin-coating technique. Specifically, films were obtained from the compound with general chemical formula: $Zn_{1-x-z}Co_xCu_zO$, [(x; z) = (0.00; 0.00), (0.02; 0.02), (0.04; 0.04) and (0.06; 0.06)]. We focused on the study of the simultaneous addition of Co and Cu cations on the morphological, structural, and optical linear and non-linear properties (second-degree refractive index and third-degree electrical susceptibility). Our study aims to amplify the optical applications of these films, specifically, in the transparent conductor screen.

2 Experimental method

2.1 Method of preparation

For synthesis, we used the general chemical formula: $Zn_{1-x-z}Co_xCu_zO$, [(x; z) = (0.00; 0.00), (0.02; 0.02), (0.04; 0.04) and (0.06; 0.06)].We prepared a solution of initial concentration (C_T = 0.5 M) and initial volume (V_T = 10ml). The raw materials, Zinc acetate dehydrates [Zn $(CH_3COO)_2 2H_2O$], Cobalt (II) chloride dihydrate ($CoCl_2.H_2O$), and Copper (II) chloride dihydrate ($CuCl_2.H_2O$) were dissolved in 2-propanol by constant agitation. The Monoethanolamine (MEA) was used as a stabilizer in the solution. The solution was mixer at 65°C for 2 h and then left for 24 h at room temperature. The glass substrates were cleaned with ethanol and acetone for 10 min and dried. The sol was transformed in crystalline films using the spin coating technique (3000 rpm), with a heat treatment at 250 °C for 4 min to steam the solvents and organic residuum and then, at 500 °C. All samples were prepared under the same conditions, respecting the mixing at the atomic level.

2.2 Characterization method

The morphologies of the films were studied from images obtained in a FEI quanta FEG 200 (FESEM) field-emitting scanning electron microscope (30 kV) and equipped with an energy-dispersion X-ray (EDAX). The XRD patterns were measurement using a Rigaku Ultima IV diffractometer in the Bragg–Brentano configuration utilizing CuKα radiation (λ = 1.54060 Å). The optical properties were analyzed by measurement obtained in a UV–visible spectrophotometer, Lambda 35 model (range of 300–800 nm). The transmission (T) and absorption (A) ranges are steeped, while the reflectance (R) is calculated using the formula: R = 1 − (T + A). Finally, the film thickness is measured by using the Claw-Tencor Alpha-Step D-500 stylus profiler.

3 Results and discussion

3.1 Morphology and chemical analysis

The morphology of the Co/Cu co-doped films are shown in Fig. 1a–d. It is evident from the images that, the surface morphology of the ZnO films is significantly assumed by deposition method and annealing time. The obtained films are composed of small spherical grains

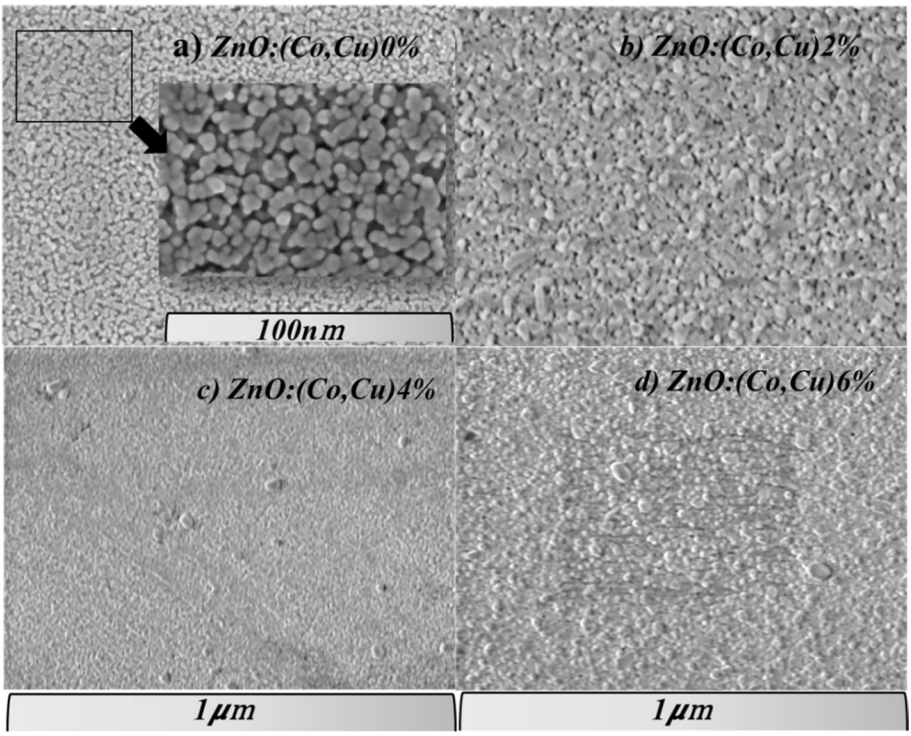

Fig. 1 SEM images of (Co–Cu) co-doped ZnO thin films **a** x = 0%, **b** x = 2%, **c** x = 4% and **d** x = 6% as a function of (Co–Cu) contents

that present interstitial spaces; more apparent for the pure ZnO film. For co-doped films, it is notable that the interstitial spaces decrease, which may be an effect of the dopant cations that help to improve the films densification. On the other hand, the EDAX analysis was performed to determine the elements composition of the obtained films, (Fig. 2a–d). As observed, all films contain the Zn and O elements, while in the co-doped ZnO films, the cobalt (Co) and copper (Cu) elements are also observed (Figs. 2b–d), confirming its insertion in the ZnO crystal structure.

3.2 Structural characterization

Figure 3 displays the X-ray diffraction patterns of the prepared films. Note that, all films have a well crystalline wurtzite hexagonal structure, typical of zinc oxide; that has been confirmed by the crystallographic card (*JCPDS No. 36-1451*). In addition, no additional phase of: Co, Cu, CuO, Cu_2O, Co_2O_4 and Co_3O_4 was observed in the XRD spectra (Goktas

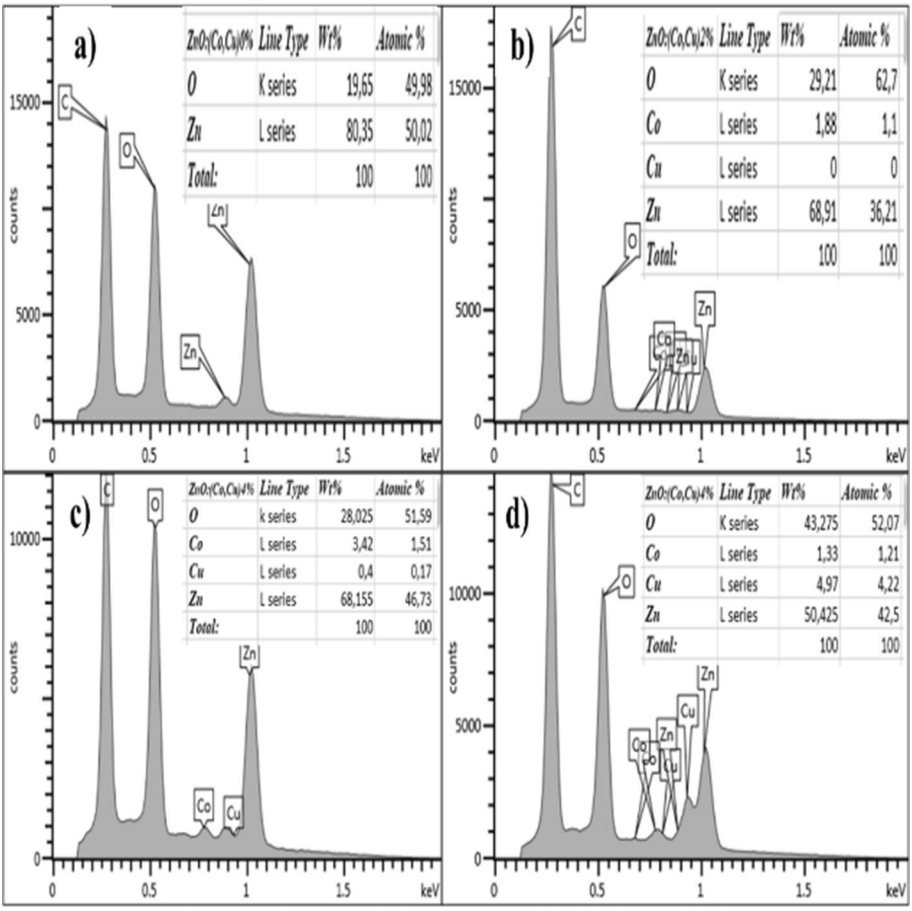

Fig. 2 EDAX spectra and table of concentration of (Co–Cu) co-doped ZnO thin films **a** x = 0%, **b** x = 2%, **c** x = 4% and **d** x = 6% as a function of (Co–Cu) contents

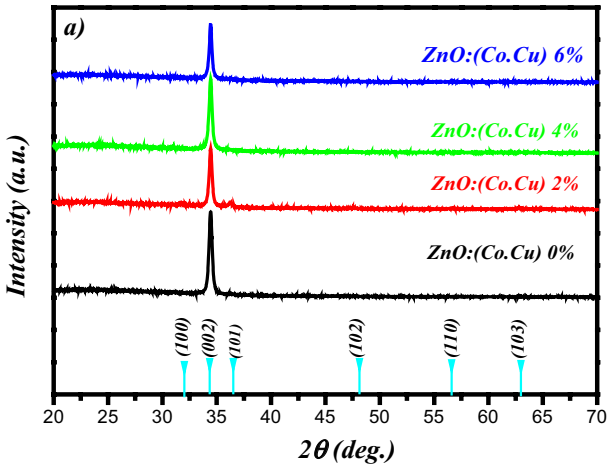

Fig. 3 **a** XRD patterns of (Co–Cu) co-doped ZnO thin films **a** x = 0%, **b** x = 2%, **c** x = 4% and **d** x = 6% as a function of (Co–Cu) contents

2018). It is important to emphasize that all films present a preferential orientation in the (002) direction. Many researchers believe that the more stable crystals level, as well as, the minimum free energy of surface, for ZnO films, is associated to the (002) plane (Mhamdi et al. 2013; Baghdad et al. 2017).

The crystal lattice parameter, (*c*) (Lupan et al. 2010), crystallite size (*D*) (Sengupta et al. 2013), dislocation density (δ) (Williamson and Smallman 1956), strain (ε_c) and stress (σ_c) (Mia et al. 2017; Muchuweni et al. 2017) were obtained using the subsequent formulas:

$$d_{hkl} = \frac{\lambda}{2\sin}, \frac{1}{d_{hkl}^2} = \frac{4}{3}\left(\frac{h^2 + hk + k^2}{a^2}\right) + \frac{l^2}{c^2} \tag{1}$$

$$u = \frac{a^2}{3c^2} + \frac{1}{4}, L = \sqrt{(\frac{a^2}{3} + (\frac{1}{2} - u)^2 c^2)} \tag{2}$$

$$D = \frac{0.9\lambda}{(\beta^2{}_{obs} - \beta^2{}_{ins})^{1/2} cos\theta}, \delta = \frac{1}{D^2} \tag{3}$$

Here λ is the X-ray wavelength (λ_{CuK_α}=1.54060 Å), $\beta = (\beta^2{}_{obs} - \beta^2{}_{ins})^{1/2}$ is the full width of the peak at half maximum (*FWHM*) once corrected in radians and θ is the Bragg diffraction angle.

$$\varepsilon_c = \frac{Cfilm - Cbulk}{Cbulk} 100\%, \sigma_c = -2.33 \times 10^{11}\left(\frac{C_{film} - C_{bulk}}{C_{bulk}}\right) \tag{4}$$

where c_{film} and $c_{bulk,}$ are the lattice parameters of the prepared films and bulk ZnO, respectively.

As shown in Table 1, the lattice parameter (*c*) values for co-doped films are inferior to the obtained for pure ZnO films. The results were influenced by the difference between the ionic radius of copper (r_{Cu+2} = 0.72Å) and that of cobalt (r_{Co+2} = 0.65Å), compared to the zinc (r_{Zn+2} = 0.74Å) (Sreedhar et al. 2016; Benzitouni et al. 2017). In addition, we note that the Co and Cu inclusion in the ZnO structure increased the

Table 1 The peak position 2θ, FWHM, lattice parameter (a and c), grain size (D), dislocation density (δ), strain (ε_c) and stress (σ_c) of the (Co–Cu) co-doped ZnO thin films

Samples	2θ(deg.)	FWHM	c(Å)	D(nm)	$\delta(10^{-3}/nm^2)$	ε_c (10^{-3})	σ_c(GPa)
Un-doped ZnO	34.414	0.330	5.205	25.140	1.582	0.1096	−0.2554
ZnO:Co 2%:Cu 2%	34.431	0.302	5.203	28.701	1.213	1.258	−0.147
ZnO:Co 4%:Cu 4%	34.436	0.301	5.202	28.131	1.263	1.254	−0.114
ZnO:Co 6%:Cu 6%	34.425	0.252	5.204	34.472	0.841	1.050	−0.186

crystalline size, ranging from 26.276 nm for the pure ZnO film to 34.472 nm for the 6% Co–Cu co-doped ZnO film. This result could be attributed to the fact that, the co-doping may have ameliorated the crystal goodness, favoring the growth and nucleation mechanisms (Narayanan and Deepak 2018; Kaphle and Hari 2018). In addition, the crystallite size increase may be related to the fact that the films have preferential orientation in the c-axis. On the other hand, we note variations in the strain values, increasing the Co–Cu dopants concentration ratios. Finally, negative stress values point that the crystal structure is in a stress state due to the dopant atoms influence, obtaining method and temperature, as well as the variance in thermal coefficient factor between the film and substrate (Joshi et al. 2016).

3.3 Optical characterization

Figure 4 exhibits the optical transmittance and reflectance spectra of the pure and co-doped ZnO films**.**In the visible spectrum, the optical transmittance of co-doped films is relatively low, compared to the pure ZnO film; around of 42% for the film co-doped at 2% and 85% for pure ZnO film. For wavelengths less than of 400 nm, the transmittance decreases rapidly, which confirms that films have shift absorption. The optical absorption coefficient $\alpha(\lambda)$ was determined for various photon energies using the transmission spectra and the equation (Gumus et al. 2006):

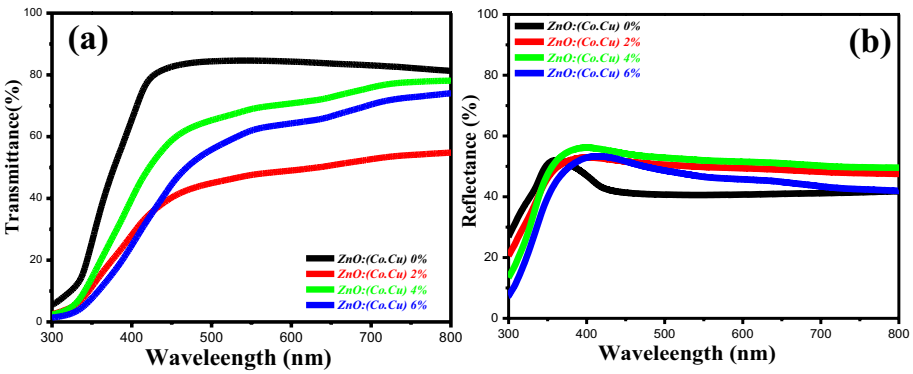

Fig. 4 **a** Optical transmittance and **b** reflectance of (Co–Cu) co-doped ZnO thin films as a function of wavelength

$$\alpha = \frac{\mathrm{Ln}(\frac{1}{T})}{t} \tag{5}$$

Here T is the transmittance and t, is the thickness of the films, that is equal to 150 nm in our case. The ZnO is a direct gap semiconductor. Thus, its energy-gap(E_g) could be deduced from the x interception of the linear extrapolation of the curve $(ahv)^2$ as a function of photon energy radiation ($h\nu$) (inset of Fig. 5) by the Tauc's relationship (Kaphle and Hari 2018):

$$(\alpha h\upsilon)^{n} = B(h\upsilon - Eg) \tag{6}$$

where B is a constant and n = 2, is used for the direct-gap energy.

In Fig. 5, the energy band-gap values (E_g) are presented as a function of Co–Cu dopants concentration. We can observe that the energy band gap decreases linearly increasing the Co–Cu concentration (3.37–3.16 eV for Co–Cu concentration ranging from 0.00 to 0.06). The energy-gap decrease can be explained by the atomic disorder (oxygen vacancy and zinc interstitial defects) generated in the ZnO structure due to the dopant cations inclusion. The defects provoke free electrons, with minor energy than the ZnO in the valence band, generating others electronic levels in the ZnO band gap, which will contribute to the energy band gap band reduction. In addition, some authors, attribute the variation in the energy gap to the charge transfer between the 4f level electrons and the conduction band or valence band of ZnO (Diouri et al. 1985; Elilarassi and Chandrasekaran 2010; Li et al. 2011). On the other hand, the small variance in the electronegativity between Cu (1.9), Co (1.88) and Zn (1.65) cations can also lead to a narrowing of the energy band gap (Ferhat et al. 2009).

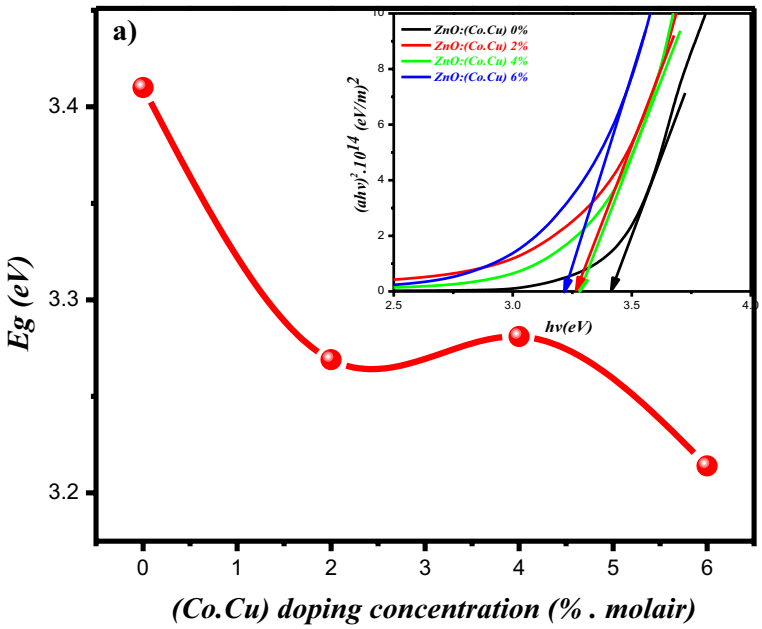

Fig. 5 **a**: Plot of $(\alpha h\upsilon)^2$ versus ($h\upsilon$) **b**: band-gap energy versus (Co–Cu) concentration

3.3.1 Linear optical parameters

The extinction coefficient (k), refractive index (n), real and imaginary parts (ε_r *and* ε_i) of the dielectric constant and optical conductivity (σ_{opt}) (Islma and Podder 2009; Caglar et al. 2007, 2008) have been calculated as follows:

$$k = \frac{\alpha\lambda}{4\pi} \tag{7}$$

$$n = \left(\frac{1+R}{1-R}\right) + \sqrt{\frac{4R}{(1-R)^2} - k^2} \tag{8}$$

$$\varepsilon_r = n^2 - k^2\varepsilon_i = 2nk \tag{9}$$

$$\sigma_{opt} = \frac{\omega}{4\pi}\sqrt{\varepsilon_i^2 + (1-\varepsilon_r)^2} \tag{10}$$

where $\omega = h\nu/\hbar\lambda$, α is the absorption coefficient and R represents the optical reflectance. The optical constants versus the wavelength are shown in Fig. 6. It is to be noted that in the visible field n is 1.75 for ZnO. This value increases for co-doped samples until it reaches about 2.5. Similar results have been reported in the literature by other authors (Hamidi et al. 2018; Istrate et al. 2019). Because of weak absorption, K is almost non-existent. The values of ε_r vary between 3 and 6 and the values of ε_i are almost zero. It can be said that the electric charge polarization varies with the electric range variation of incident wave. We also note an enhancement in the refractive index, damping factor, and the imaginary part appearance. This is owing to the attendance of great absorption and electron transfer in ultraviolet fields (Mahdhi et al. 2018).

On the other hand, the Fig. 7a displays the change of optical conductivity for the Co–Cu co-doped ZnO films in terms of the wavelength. As observed, the conductivity changes are like those of the absorption and the imaginary part of the dielectric constant. In addition, the optical conductivity was deduced in terms of the Co–Cu dopant percentages and are shown in Fig. 7b. Note that the optical conductivity values vary between 1.68×10^{16} and 1.30×10^{16} (1/s). Compared to the previous report, for Cu-doped ZnO thin films, there was an improvement due to the simultaneous Co and Cu dopant cations insertion in the ZnO crystal structure (Mohammedi et al. 2021).

The refractive index at elevated frequencies (n_∞^2) (Walton and Moss 1963), the individual oscillator energy of electronic transitions (E_0) and the dispersal energy (E_d) (Caglar et al. 2007) were calculated using the following equations:

$$\frac{n_\infty^2 - 1}{n^2 - 1} = 1 - \left(\frac{\lambda_0}{\lambda}\right)^2 \tag{11}$$

$$n^2 = 1 + \frac{E_d E_0}{E_0^2 + (h\nu)^2} \tag{12}$$

Plotting $(n_\infty^2 - 1)^{-1}$ in terms of λ^{-2}, the value of the n_∞^2 may be deduced from the intersection with the ordinal axis of Fig. 8a. Plotting $(n^2 - 1)^{-1}$ in terms of $(h\nu)^2$, the values of

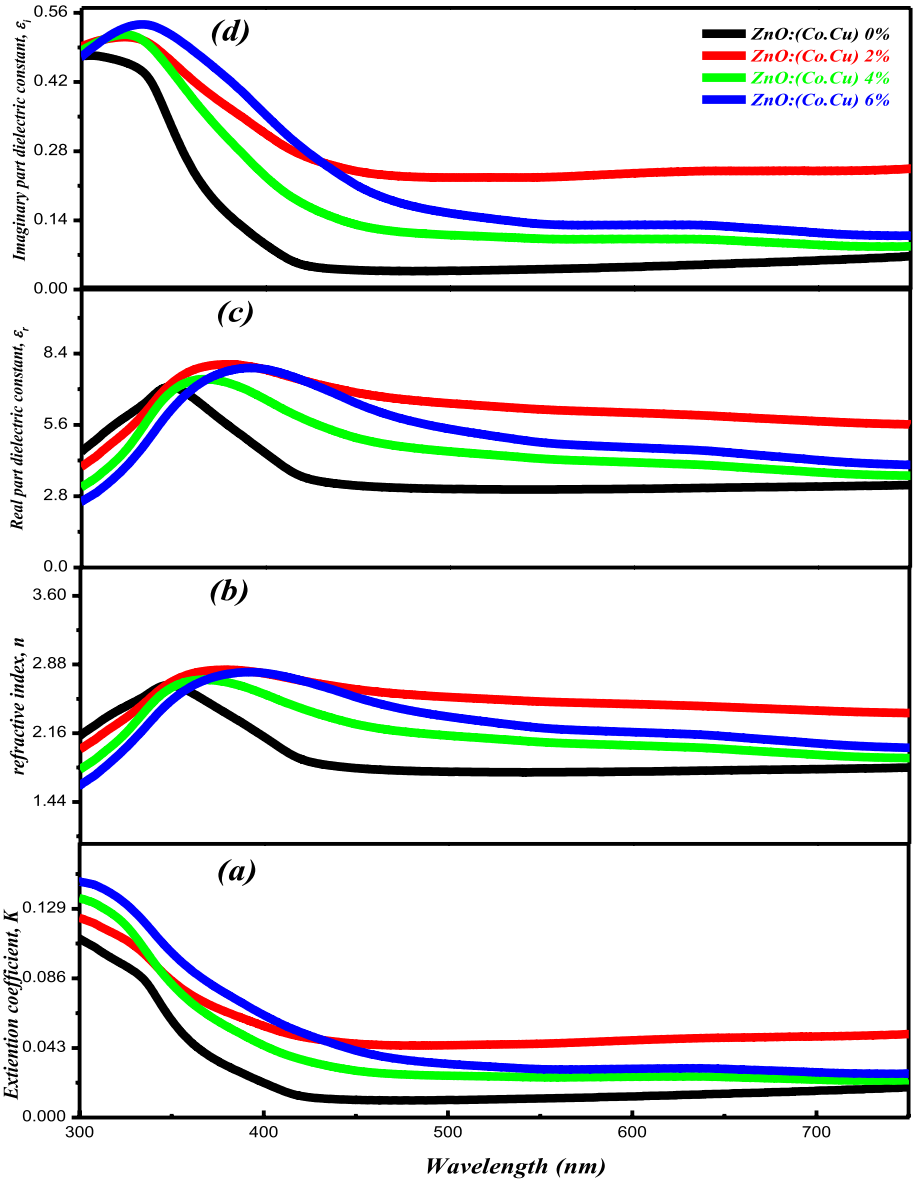

Fig. 6 **a**: Refractive index n, **b**: extinction coefficient k, **c**: real part of dielectric constant $\varepsilon_r$and **d**: imaginary part of dielectric constant $\varepsilon_i$of the (Co–Cu) co-doped ZnO thin films with various wavelengths

E_0 and E_d can be calculated by intersecting the order axis and the slope as shown in Fig. 8. The E_0, E_d and n_∞ values for the Co–Cu co-doped ZnO thin films are illustrated in the Table 2. Note that the values of E_d and n_∞ are improved increasing the Co–Cu concentration and these results are almost consistent for reported by Gao Xiao-Yong et al. (Gao et al. 2010). All the values of E_0 of the doped films are higher than that of the undoped film; on the other hand, E_0 decreases with the increase of the doping concentration.

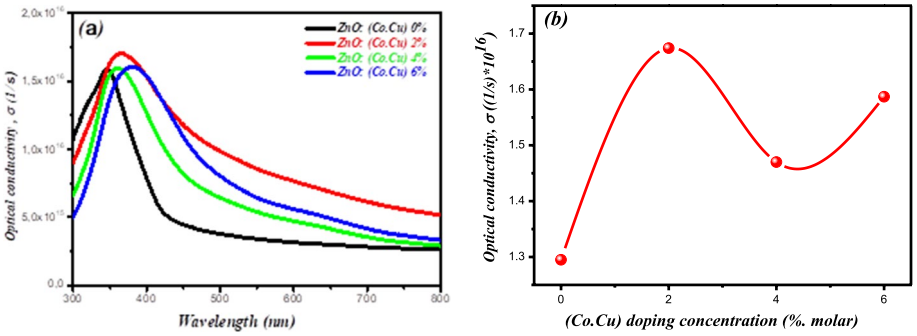

Fig. 7 Optical conductivity of (Co–Cu)co-doped ZnO, **a**: versus wavelength and **b**: versus Co–Cu concentration

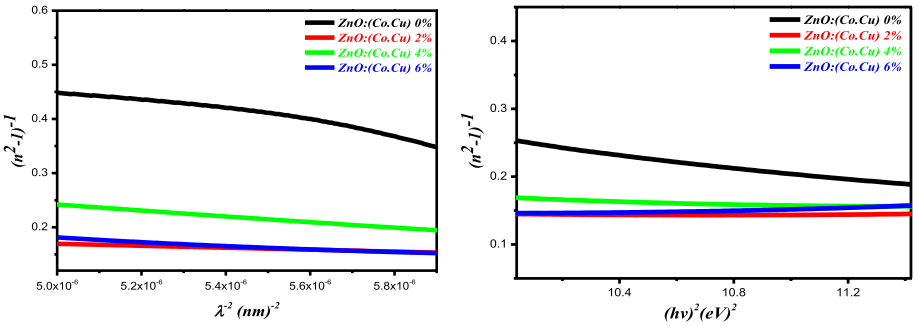

Fig. 8 **a**: The plot of $(n^2-1)^{-1}$ various $(\lambda)^{-2}$ and **b**: the plot of $(n^2-1)^{-1}$ various $(hv)^2$ of the (Co–Cu) co-doped ZnO thin films

Table 2 Optical dispersion parameters of (Co–Cu) co-doped ZnO thin films

Samples	E_0 (eV)	E_d (eV)	$\varepsilon i = n_\infty^2$
Un-doped ZnO	4.216	5.929	3.227
ZnO:Co 2%:Cu 2%	6.899	14.494	6.882
ZnO:Co 4%:Cu 4%	5.513	18.136	5.132
ZnO:Co 6%:Cu 6%	4.949	20.203	6.524

3.3.2 Nonlinear optical parameters

The investigation of the interaction of the electromagnetic field with the physical medium, where the interaction of the electric field with the incidental wave is of non-linear polarization is shown by the subsequent formula (Frumar et al. 2003)

$$P_{NL} = \chi^{(1)}E + \chi^{(2)}\mathrm{E2} + \ldots \chi^{(n)}E^n \tag{13}$$

Here, $\chi^{(1)}$, $\chi^{(2)}$ E^2 and $\chi^{(3)}$ E^3 are the polarizabilities, $\chi^{(1)}$ is the linear optical susceptibility, and $\chi^{(2)}$ and $\chi^{(3)}$ are the second- and third-order nonlinear optical susceptibility, respectively.

The n becomes non-linear according to the following equation,

$$n(\lambda) = n_0(\lambda) + n^{(2)}\left(E^2\right) \tag{14}$$

Here , $n^{(0)}$ is linear, n and $n^{(2)}$ is nonlinear. The n is allied to the electric field power. Various quasi-empirical equations are nominated to calculate the third-order non-linear optical susceptibility $\chi^{(3)}$ and the non-linearn$^{(2)}$. Amongst these relations, one may obtain the Miller formula generalized in the subsequent relation (Ticha and Tichy 2002),

$$\chi^{(3)} = A(\chi^{(1)}) \tag{15}$$

According to Adair et al. (Ferhat et al. 2009), the valueof the constant (A) is equal to 1.79×10^{-10}(for $\chi^{(1)}$ in esu). For a different type of materials,

$$\chi^{(1)} = \frac{(n^2 - 1)}{4\pi} \tag{16}$$

Considering the Eq. (13), at small frequencies hv$\rightarrow$0 and n = n_0, ($\chi^{(1)}$) is explained by:

$$\chi^{(1)} = \frac{E_d}{E_0 4\pi} \tag{17}$$

$$n^{(2)} = \frac{12\pi\chi^{(3)}}{n_0} \tag{18}$$

We have calculated the quantities of $\chi^{(1)}$, $\chi^{(3)}$ and $n^{(2)}$ in terms of the wavelength (Fig. 9a–c). We notice that the values of these parameters increase in the ultraviolet field, but they are almost constant in the visible field. The NLO constants values increase with the Co–Cu co-dopant cations insertion (Table 3). This phenomenon is related to a crystallization improved of the samples (Table 1). Everything indicates that our ZnO thin films co-doped with Co and Cu are candidate for NLO applications.

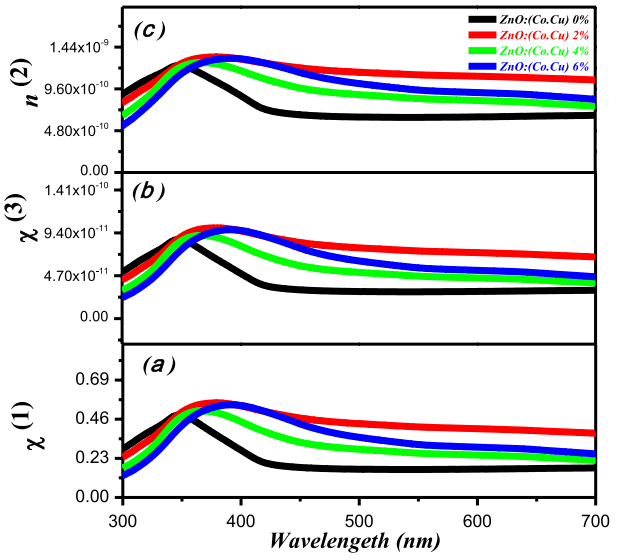

Fig. 9 **a**: Linear optical susceptibility $\chi^{(1)}$, **b**: third order nonlinear susceptibility $\chi^{(3)}$, and **c**: nonlinear refractive index $n^{(2)}$ of the (Co–Cu) co-doped ZnO as a function of wavelength

Table 3 Nonlinear optical parameters of reported and present work on ZnO thin films

Samples	n_0	$\chi^{(1)}$	$\chi^{(3)}$, esu	$n^{(2)}$, esu
Un-doped ZnO (present work)	1.815	0.111	2.004×10^{-11}	4.161×10^{-10}
ZnO:Co 2%:Cu 2%(present work)	2.346	0.167	2.994×10^{-11}	4.808×10^{-10}
ZnO:Co 4%:Cu 4% (present work)	1.894	0.261	4.688×10^{-11}	9.326×10^{-10}
ZnO:Co 6%:Cu 6% (present work)	1.976	0.324	5.816×10^{-11}	1.109×10^{-9}
Co-doped ZnO Shaaban et al. (2016)	–	0.13–0.20	$0.48–2.72\times0^{-13}$	$1.89–9.11\ 9\times10^{-10}$
Sn-doped ZnO Ganesh et al. (2017)	–	0.1–0.91	$0.51–9.09\times10^{-11}$	$0.5\times10^{-10}–1\times10^{-9}$
Cu-doped ZnO Ganesh et al. (2018)	–	0.09–0.19	$0.25–2.25\times10^{-13}$	$0.25–4.59\times10^{-12}$

4 Conclusions

In the present study, thin films of ZnO co-doped with cations of Co^{2+} and Cu^{2+} were obtained utilizing the sol–gel method and spin coating technique. The morphological, structural, and optical linear and nonlinear properties are analyzed in detail. The SEM images revealed that the pure ZnO film is composed by small spherical grains that present interstitial spaces, while the films obtained from the simultaneous Co and Cu insertion in the ZnO structure are more dense and interstitial spaces disappear. The EDAX data confirm the attendance of Co, Cu, Zn and O elements in the ZnO thin films. The X-ray diffraction patterns confirmed the single-phase formation of ZnO and preferential orientation in the (002) direction. In addition, the Zn^{2+} cations by Co^{2+} and Cu^{2+} cations replacement, provokes significant variations in the lattice parameter (c), crystallite size (D), dislocation density (δ), strain (ε_c) and stress (σ_c) of the hexagonal structure wurtzite from ZnO. In general, the results obtained in this work provide new alternatives for designing thin films with optoelectronics applications. This is because the layers have the desired nonlinear optical properties to effectively transparent conductive screens.

Author contributions AM: Performed the experiences of this work. OM: Performed the experiences of this work. MI: Supervised and developed the experience. BM and RP-G: Verified the development of experiences. NB: Supervised the findings of this work. All authors discussed the results and contributed to the final manuscript.

Funding No funding was received to assist with the preparation of this manuscript.

Declarations

Conflict of interest The authors declare that they have no conflicts of interest.

References

Ali, R.N., Naz, H., Li, J., Zhu, X., Liu, P., Xiang, B.: Band gap engineering of transition metal (Ni/Co) codoped in zinc oxide (ZnO) nanoparticles. J. Alloy. Compd. **744**, 90–95 (2018)

Andriotis, A.N., Menon, M.: Band gap engineering via doping: a predictive approach. J. Appl. Phys. **117**, 125708 (2015)

Baghdad, R., Lemée, N., Lamura, G., Zeinert, A., Hadj-Zoubir, N., Bousmaha, M., Bezzerrouk, M., Bouyanfif, H., Allouche, B., Zellama, K.: Structural and magnetic properties of Co-doped ZnO thin films grown by ultrasonic spray pyrolysis method. Superlattices Microstruct. **104**, 553–569 (2017)

Bahedi, K., Addou, M., El Jouad, M., Bayoud, S., Sofiani, Z.: Effects of deposition temperature on the surface roughness and the nonlinear optical susceptibility of sprayed deposited ZnO: Zr thin films. Appl. Surf. Sci. **255**, 9054–9057 (2009a)

Bahedi, K., Addou, M., El Jouad, M., Sofiani, Z., Lamrani, M.A., El Habbani, T., Fellahi, N., Bayoud, S., Dghoughi, L., Sahraoui, B.: Diagnostic study of the roughness surface effect of zirconium on the third-order nonlinear-optical properties of thin films based on zinc oxide nanomaterials. Appl. Surf. Sci. **255**, 4693–4695 (2009b)

Benzitouni, S., Zaabat, M., Ebothe, J., Boudine, B., Coste, R.: The use of advanced atomic force microscopy for the quantitative nanomechanical characterization of Co-doped ZnO thin films. Chin. J. Phys. **55**, 2458–2467 (2017)

Caglar, Y., Ilican, S., Caglar, M.: Single-oscillator model and determination of optical constants of spray pyrolyzed amorphous SnO 2 thin films. Eur. Phys. J. B **58**, 251–256 (2007)

Caglar, M., Ilican, S., Caglar, Y., Yakuphanoglu, F.: The effects of Al doping on the optical constants of ZnO thin films prepared by spray pyrolysis method. J. Mater. Sci.: Mater. Electron. **19**, 704–708 (2008)

Chaitra, U., Kekuda, D., Rao, K.M.: Effect of annealing temperature on the evolution of structural, microstructural, and optical properties of spin coated ZnO thin films. Ceram. Int. **43**, 7115–7122 (2017)

Chen, Z.-W., Yao, C.-B., Han, Y., Bao, S.-B., Jiang, G.-Q., Cai, Y.: Synthesis, structure and femtosecond nonlinear absorption properties of Ce-ZnO films. Appl. Surf. Sci. **502**, 144133 (2020)

Chouhan, R., Baraskar, P., Agrawal, A., Gupta, M., Sen, P.K., Sen, P.: Effects of oxygen partial pressure and annealing on dispersive optical nonlinearity in NiO thin films. J. Appl. Phys. **122**, 025301 (2017)

Costa-Silva, M., Araujo, F.P., Guerra, Y., Viana, B.C., Silva-Filho, E.C., Osajima, J.A., Almeida, L.C., Skovroinski, E., Peña-Garcia, R.: Photocatalytic, structural and optical properties of Ce–Ni co-doped ZnO nanodisks-like self-assembled structures. Mater. Chem. Phys. **292**, 126814 (2022)

El Hamidi, A., Meziane, K., El Hichou, A., Jannane, T., Liba, A., El Haskouri, J., Amorós, P., Almaggoussi, A.: Refractive index controlled by film morphology and free carrier density in undoped ZnO through sol-pH variation. Optik **158**, 1139–1146 (2018)

Deekshitha, U., Upadhya, K., Antony, A., Ani, A., Nowak, M., Kityk, I., Jedryka, J., Poornesh, P., Manjunatha, K.: Effect of Na doping on photoluminescence and laser stimulated nonlinear optical features of ZnO nanostructures. Mater. Sci. Semicond. Process. **101**, 139–148 (2019)

Diouri, J., Lascaray, J., El Amrani, M.: Effect of the magnetic order on the optical-absorption edge in Cd 1–x Mn x Te. Phys. Rev. B **31**, 7995 (1985)

Elilarassi, R., Chandrasekaran, G.: Structural, optical and magnetic characterization of Cu-doped ZnO nanoparticles synthesized using solid state reaction method. J. Mater. Sci.: Mater. Electron. **21**, 1168–1173 (2010)

Ferhat, M., Zaoui, A., Ahuja, R.: Magnetism and band gap narrowing in Cu-doped ZnO. Appl. Phys. Lett. **94**, 142502 (2009)

França, R., Araujo, F.P., Neves, L., Melo, A., Lins, A., Soares, A.S., Osajima, J.A., Guerra, Y., Almeida, L.C., Peña-Garcia, R.R.: Photoresponsive activity of the Zn0. 94Er0. 02Cr0. 04O compound with hemisphere-like structure obtained by Co-precipitation. Materials **16**, 1446 (2023)

Frumar, M., Jedelský, J., Frumarova, B., Wagner, T., Hrdlička, M.: Optically and thermally induced changes of structure, linear and non-linear optical properties of chalcogenides thin films. J. Non-Cryst. Solids **326**, 399–404 (2003)

Ganesh, V., Salem, G., Yahia, I., Yakuphanoglu, F.: Synthesis, optical and photoluminescence properties of Cu-doped ZnO nano-fibers thin films: nonlinear optics. J. Electron. Mater. **47**, 1798–1805 (2018)

Ganesh, V., Yahia, I., AlFaify, S., Shkir, M.: Sn-doped ZnO nanocrystalline thin films with enhanced linear and nonlinear optical properties for optoelectronic applications. J. Phys. Chem. Solids **100**, 115–125 (2017)

Gao, X.-Y., Feng, H.-L., Ma, J.-M., Zhang, Z.-Y., Lu, J.-X., Chen, Y.-S., Yang, S.-E., Gu, J.-H.: Analysis of the dielectric constants of the Ag2O film by spectroscopic ellipsometry and single-oscillator model. Physica B **405**, 1922–1926 (2010)

Goktas, A.: High-quality solution-based Co and Cu co-doped ZnO nanocrystalline thin films: comparison of the effects of air and argon annealing environments. J. Alloy. Compd. **735**, 2038–2045 (2018)

Gumus, C., Ozkendir, O., Kavak, H., Ufuktepe, Y.: Structural and optical properties of zinc oxide thin films prepared by spray pyrolysis method. J. Optoelectron. Adv. Mater. **8**, 299 (2006)

Hadimani, P., Ghosh, S., Sil, A.: Preparation of Fe doped ZnO thin films and their structural, magnetic, electrical characterization. Superlattices Microstruct. **120**, 199–208 (2018)

Islam, M., Podder, J.: Optical properties of ZnO nano fiber thin films grown by spray pyrolysis of zinc acetate precursor. Crystal Res. Technol. J. Exp. Ind. Crystallogr. **44**, 286–292 (2009)
Islam, M.R., Rahman, M., Farhad, S., Podder, J.: Structural, optical and photocatalysis properties of sol–gel deposited Al-doped ZnO thin films. Surf. Interfaces **16**, 120–126 (2019)
Istrate, A.-I., Nastase, F., Mihalache, I., Comanescu, F., Gavrila, R., Tutunaru, O., Romanitan, C., Tucureanu, V., Nedelcu, M., Müller, R.: Synthesis and characterization of Ca doped ZnO thin films by sol–gel method. J. Sol-Gel. Sci. Technol. **92**, 585–597 (2019)
Joshi, K., Rawat, M., Gautam, S.K., Singh, R., Ramola, R., Singh, F.: Band gap widening and narrowing in Cu-doped ZnO thin films. J. Alloy. Compd. **680**, 252–258 (2016)
Kaphle, A., Hari, P.: Enhancement in power conversion efficiency of silicon solar cells with cobalt doped ZnO nanoparticle thin film layers. Thin Solid Films **657**, 76–87 (2018)
Kim, Y., Choe, J., Nam, G., Kim, I., Leem, J.-Y., Lee, S.-H., Kim, S., Kim, D.Y., Kim, S.-O.: Influence of Al-, Co-, Cu-, and In-doped ZnO buffer layers on the structural and the optical properties of ZnO thin films. J. Korean Phys. Soc. **66**, 224–228 (2015)
Kompa, A., Devi, B.L., Chaitra, U.: Determination of optical constants of vacuum annealed ZnO thin films using Wemple Di Domenico model Sellmier's model and Miller's generalized rules. Mater. Chem. Phys. **299**, 127507 (2023)
Li, X.-Y., Li, H.-J., Yuan, M., Wang, Z.-J., Zhou, Z.-Y., Xu, R.-B.: Influence of oxygen partial pressure on electrical and optical properties of Zn0. 93Mn0. 07O thin films. J. Alloys Compd. **509**, 3025–3031 (2011)
Lupan, O., Pauporté, T., Chow, L., Viana, B., Pellé, F., Ono, L.K., Cuenya, B.R., Heinrich, H.: Effects of annealing on properties of ZnO thin films prepared by electrochemical deposition in chloride medium. Appl. Surf. Sci. **256**, 1895–1907 (2010)
Mahdhi, H., Djessas, K., Ayadi, Z.B.: Synthesis and characteristics of Ca-doped ZnO thin films by rf magnetron sputtering at low temperature. Mater. Lett. **214**, 10–14 (2018)
Mahroug, A., Mari, B., Mollar, M., Boudjadar, I., Guerbous, L., Henni, A., Selmi, N.: Studies on structural, surface morphological, optical, luminescence and UV photodetection properties of sol–gel Mg-doped ZnO thin films. Surf. Rev. Lett. **26**, 1850167 (2019)
Mhamdi, A., Boukhachem, A., Madani, M., Lachheb, H., Boubaker, K., Amlouk, A., Amlouk, M.: Study of vanadium doping effects on structural, opto-thermal and optical properties of sprayed ZnO semiconductor layers. Optik-Int. J. Light Electron Opt. **124**, 3764–3770 (2013)
Mia, M.N.H., Pervez, M.F., Hossain, M.K., Rahman, M.R., Uddin, M.J., Al Mashud, M.A., Ghosh, H.K., Hoq, M.: Influence of Mg content on tailoring optical bandgap of Mg-doped ZnO thin film prepared by sol-gel method. Results Phys. **7**, 2683–2691 (2017)
Mohammedi, A., Ibrir, M., Meglali, O., Berri, S.: Influence of Cu-doping on linear and nonlinear optical properties of high-quality ZnO thin films obtained by spin-coating technique. Physica Status Solidi (b) **258**, 2000472 (2021)
Mohammedi, A., Ibrir, M., Meglali, O., Pena-Garcia, R.: Effect of annealing of Co-Doped ZnO thin films on structural and magnetic properties deposited by sol–gel/spin-Coating technique. Surf. Rev. Lett. **29**, 2230007 (2022)
Mostafa, A.M., Mwafy, E.A., Awwad, N.S., Ibrahium, H.A.: Linear and nonlinear optical studies of Ag/Zn/ZnO nanocomposite thin film prepared by pulsed laser deposition technique. Radiat. Phys. Chem. **179**, 109233 (2021)
Muchuweni, E., Sathiaraj, T., Nyakotyo, H.: Synthesis and characterization of zinc oxide thin films for optoelectronic applications. Heliyon **3**, e00285 (2017)
Nagaraja, K., Pramodini, S., Kumar, A.S., Nagaraja, H., Poornesh, P., Kekuda, D.: Third-order nonlinear optical properties of Mn doped ZnO thin films under cw laser illumination. Opt. Mater. **35**, 431–439 (2013)
Narayanan, N., Deepak, N.: Enhancement of visible luminescence and photocatalytic activity of ZnO thin films via Cu doping. Optik **158**, 1313–1326 (2018)
Oudjertli, S., Mohammedi, A., Ibrir, M.: Effect of Ni doping on the optical properties of ZnO thin films prepared by sol-gel spin coating and investigation of ZnO powder nanostructures. Solid State Phenom. **336**, 103–107 (2022)
Peng, Y., Wang, G., Yuan, C., He, J., Ye, S., Luo, X.: Influences of oxygen vacancies on the enhanced nonlinear optical properties of confined ZnO quantum dots. J. Alloy. Compd. **739**, 345–352 (2018)
Peña-Garcia, R., Guerra, Y., Milani, R., Oliveira, D., Rodrigues, A., Padrón-Hernández, E.: The role of Y on the structural, magnetic and optical properties of Fe-doped ZnO nanoparticles synthesized by sol gel method. J. Magn. Magn. Mater. **498**, 166085 (2020)

Peña-Garcia, R., Guerra, Y., Milani, R., Oliveira, D., de Souza, F., Padrón-Hernández, E.: Influence of Ni and Sr on the structural, morphological and optical properties of ZnO synthesized by sol gel. Opt. Mater. **98**, 109427 (2019)
Rocha, M., Araujo, F.P., Castro-Lopes, S., de Lima, I.S., Silva-Filho, E.C., Osajima, J.A., Oliveira, C.S., Viana, B.C., Almeida, L.C., Guerra, Y.: Synthesis of Fe–Pr co-doped ZnO nanoparticles: structural, optical and antibacterial properties. Ceram. Int. **49**, 2282–2295 (2023)
Sengupta, J., Ahmed, A., Labar, R.: Structural and optical properties of post annealed Mg doped ZnO thin films deposited by the sol–gel method. Mater. Lett. **109**, 265–268 (2013)
Shaaban, E., El-Hagary, M., Hassan, H.S., Ismail, Y.A., Emam-Ismail, M., Ali, A.: Structural, linear and nonlinear optical properties of co-doped ZnO thin films. Appl. Phys. A **122**, 1–10 (2016)
Sreedhar, A., Kwon, J.H., Yi, J., Kim, J.S., Gwag, J.S.: Enhanced photoluminescence properties of Cu-doped ZnO thin films deposited by simultaneous RF and DC magnetron sputtering. Mater. Sci. Semicond. Process. **49**, 8–14 (2016)
Swapna, P., Reddy, S.V.: Synthesis and structural properties of (Co, Al) Co-doped ZnO nanoparticles. Adv. Sci. Lett. **24**, 5636–5639 (2018)
Ticha, H., Tichy, L.: Semiempirical relation between non-linear susceptibility (refractive index), linear refractive index and optical gap and its application to amorphous chalcogenides. J. Optoelectron. Adv. Mater. **4**, 381–386 (2002)
Walton, A., Moss, T.: Determination of refractive index and correction to effective electron mass in PbTe and PbSe. Proc. Phys. Soc. **81**, 509 (1963)
Williamson, G., Smallman, R., III.: Dislocation densities in some annealed and cold-worked metals from measurements on the X-ray debye-scherrer spectrum. Phil. Mag. **1**, 34–46 (1956)
Yan, Z., Bao, J., Yue, X.-Y., Li, X.-L., Zhou, Y.-N., Wu, X.-J.: Impacts of preparation conditions on photoelectric properties of the ZnO: Ge transparent conductive thin films fabricated by pulsed laser deposition. J. Alloy. Compd. **812**, 152093 (2020)

Authors and Affiliations

Abdelkader Mohammedi[1,2] · Omar Meglali[2,3] · Miloud Ibrir[1,2] · Bernabé Marí[4] · R. Peña-Garcia[5,6] · Nadir Bouarissa[1,2]

✉ Nadir Bouarissa
n_bouarissa@yahoo.fr

Abdelkader Mohammedi
abdelkader.mohammedi@univ-msila.dz

Omar Meglali
omar.meglali@univ-msila.dz

Miloud Ibrir
miloud.ibrir@univ-msila.dz

Bernabé Marí
B_mari@yahoo.fr

R. Peña-Garcia
ramon.raudel@ufrpe.br; rraudelp@gmail.com

[1] Laboratory of Materials Physics and Its Applications, University of M'sila, 28000 M'sila, Algeria

[2] Faculty of Sciences, University of M'sila, 28009 M'sila, Algeria

[3] Materials Science and Informatics Laboratory, Ziane Achour University, Djelfa, Algeria

[4] Institut de Disseny, Fabricació I Producció Automatitzada, Universitat Politècnica de València, 46022 València, Spain

[5] Interdisciplinary Laboratory Advanced Materials (Limav), Federal University of Piauí, Teresina, PI, Brazil

[6] Federal Rural University of Pernambuco, Academic Unit of Cabo de Santo Agostinho, Cabo de Santo Agostinho, PE 54518-430, Brazil